# Identification of moving loads using the $\ell_1$ norm minimization

Michał Gawlicki, and Łukasz Jankowski

Citation: AIP Conference Proceedings **1922**, 100007 (2018);
View online: https://doi.org/10.1063/1.5019092
View Table of Contents: http://aip.scitation.org/toc/apc/1922/1
Published by the American Institute of Physics

# Identification of Moving Loads Using the $\ell_1$ Norm Minimization

Michał Gawlicki[a)] and Łukasz Jankowski[b)]

*Institute of Fundamental Technological Research, Polish Academy of Sciences*
*Pawińskiego 5B, 02-106 Warsaw, Poland*

[a)]mgawlic@ippt.pan.pl
[b)]ljank@ippt.pan.pl

**Abstract.** This contribution deals with the inverse problem of indirect identification of moving loads. The identification is performed based on the recorded response of the loaded structure and its numerical model. A specific feature of such problems is a very large number of the degrees of freedom (DOFs) that can be excited and a limited number of available sensors. As a result, unless the solution space is significantly limited, the identification problem is underdetermined: it has an infinite number of exact, observationally indistinguishable solutions. We propose an approach based on the assumption of sparsity of the excitation, which can be expressed in the form of a requirement of a bounded $l_1$ norm of the solution. As long as the loads are sparse, the approach allows them to be freely moving, without the usual assumption of a constant velocity. We first test the approach in a numerical example with 10% rms measurement noise. A good qualitative agreement of the numerical results allows to proceed with experimental investigations, and the moving load identification is then carried out based on the response measured experimentally on a lab test stand.

The two main problems in the area of structural health monitoring (SHM) are monitoring for structural damages and indirect identification of structural loads. In general terms, these problems correspond respectively to the inverse problems of the first type (system identification) and the second type (input identification).

This contribution is devoted to indirect identification of moving loads based on the recorded responses of the loaded structure. Such a problem has been intensively studied and there is a number of extensive reviews [1,2]. The problem is important in assessment of pavements and bridges, in traffic monitoring and control, as well as a prerequisite for structural control [3-6]. A specific feature of such problems is a very large number of the degrees of freedom (DOFs) that can be excited by the load and a limited number of sensors available to measure the response. As a result, unless the solution space is significantly limited, the identification problem is underposed: it has an infinite number of exact solutions. In most of the published research, the solution space is limited by the assumption of a single vehicle that moves at a constant velocity. Such approaches have led to very good results; however, they significantly restrict the generality of the load being identified and exclude, e.g., braking or accelerating vehicles, freely moving loads and multiple loads.

We propose and test an approach based on the assumption of sparsity of the excitation, which is well-tailored to practice: even if there are multiple loads, at each time instant the excitation usually occurs in a very limited number of structural DOFs. Such an approach fits into the recent intense research stream on compressed sensing [7], which includes SHM-related application areas such as damage identification [8] or identification of impact load position [9]. To our best knowledge, the concept has not been applied for identification of transient moving loads. The assumption of sparsity is usually expressed as a requirement of a bounded $l_1$ norm of the solution [10]. As long as the loads are sparse, the approach allows them to be identified even if they are multiple or freely moving, that is without the usual assumption of a constant velocity.

*Computer Methods in Mechanics (CMM2017)*
AIP Conf. Proc. 1922, 100007-1–100007-9; https://doi.org/10.1063/1.5019092
Published by AIP Publishing. 978-0-7354-1614-7/$30.00

## The Direct Problem

The structure is modelled by means of the finite element (FE) method. It is assumed to satisfy the equation of motion in its standard form with zero initial conditions:

$$\mathbf{M}\ddot{\mathbf{x}} + \mathbf{C}\dot{\mathbf{x}} + \mathbf{K}\mathbf{x} = \mathbf{f}, \quad \mathbf{x}(0) = \mathbf{0}, \quad \dot{\mathbf{x}}(0) = \mathbf{0}, \tag{1}$$

where **M**, **C** and **K** are respectively the structural mass, damping and stiffness matrices, and **f** represents the excitation by the freely moving load(s). Since the model is linear, responses of linear sensors (such as strain gauges) can be stated in the convolution form,

$$\boldsymbol{\varepsilon}(t) = \int_0^t \mathbf{B}_\mathrm{c}(t-\tau)\mathbf{f}(\tau)\,\mathrm{d}\tau, \tag{2}$$

where the matrix $\mathbf{B}_\mathrm{c}$ collects the structural impulse response functions. After time discretization, Eqn (2) takes the following form:

$$\boldsymbol{\varepsilon} = \mathbf{B}\mathbf{f}, \tag{3}$$

where the vectors $\boldsymbol{\varepsilon}$ and **f** collect all the discretized responses and excitations (for all time instances), and **B** is a block Toeplitz matrix that represents the discretized form of the convolution operator. Each block row of **B** corresponds to a single sensor, while each block column corresponds to a single excitation point.

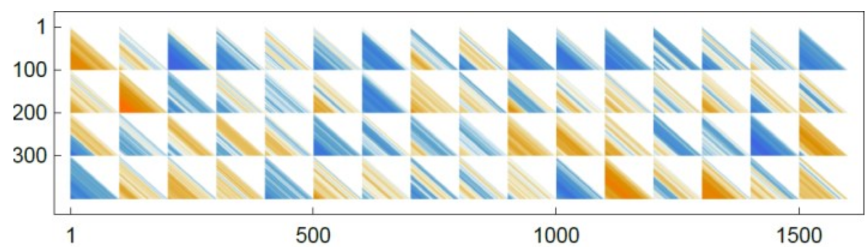


**FIGURE 1.** Example of a block matrix **B** (4x16 blocks, each block is 100x100)

## The Inverse Problem

A discrete set of points that can be crossed by the moving load is selected on the surface of the structure. The set needs to be dense enough to be able to model the load trajectory. Let the vector **p** collect force excitations in all these points and in all time instances, and let **N** be the allocation matrix which allocates the points to structural DOFs. Notice that the number of points might be smaller than the number of structural DOFs and that the points need not be aligned with specific DOFs (in such a case they are allocated to the DOFs of the involved finite elements using their shape functions). As a result, Eqn (3) takes the form

$$\boldsymbol{\varepsilon} \approx \mathbf{B}\mathbf{N}\mathbf{p}, \tag{4}$$

that is the vector **f** is approximated by assuming that the load interacts with the structure only in the considered set of points, $\mathbf{f} \approx \mathbf{N}\mathbf{p}$. In general, load identification is then equivalent to solving of Eqn (4).

## Assumption of Sparsity and the $l_1$Norm Minimization

In practical cases, there are much more potential excitation points than sensors, so that the length of the excitation vector **p** is much larger than the length of the measurement vector **ε**, so that Eqn (4) has infinitely many exact solutions. To obtain a unique solution, an additional knowledge about the load has to be used to constrain the solution space. In literature, a single load is usually assumed with known trajectory and velocity. Here, we propose an assumption of sparsity, which can be expressed through the $l_1$ norm as the task of minimization of the following weighted objective function [9]:

$$F(\mathbf{p}) = \|\boldsymbol{\varepsilon} - \mathbf{BNp}\|^2 + \alpha\|\mathbf{p}\|_1, \tag{5}$$

where the coefficient $\alpha$ weights the importance of the criterion of sparsity. The fact that the regularization with respect to the $l_1$norm promotes sparse solutions can be illustrated using the following intuitive example. The isolines of the $l_1$ norm in the $R^2$ space are presented in Fig. 2 in red colour. The subspace of all accurate solutions of a two dimensional counterpart of Eqn (4) is represented by a blue line. It can be noted that the minimum value of the $l_1$ norm within the subspace is attained when at least one component is zero.

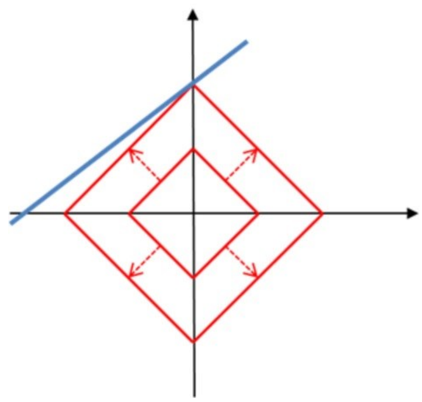

**FIGURE 2.**The isolines of the $l_1$ norm in the $R^2$ space (red). The $l_1$ minimum in a subspace (blue) is attained when at least one of the coordinates is zero

# NUMERICAL EXAMPLE

For preliminary verification of the proposed approach, a numerical example is considered. The measuring section of the actual experimental stand, Fig. 6, is numerically modelled as a 2D FE beam, see Fig. 3. The material, geometric, constraint and excitation parameters are tuned to represent the experimental setup. The beam is divided into 22 finite elements (Euler-Bernoulli beams). In each time step of the forward simulation, the moving mass load is transferred to the DOFs of the involved finite element via its shape functions. Strain sensors are assumed to be placed in four points of the beam at 20%, 40%, 60% and 80% of the beam span. In these points the strain is simulated numerically, contaminated with a 10% rms uncorrelated Gaussian noise and used in the identification procedure as measurements. The number of unknowns in Eqn (5) is thus equal to $16n_t$, and they all have to be identified based on only $4n_t$ measurements, where $n_t$ is the number of the time steps.

Geometric and material parameters of the beam are as follows: the beam 0.55m long and its cross-section is 0.03m x 0.0015m. The Young modulus is 205GPa and the density is 7800kg/m3, which corresponds to steel.

Graphical time-space representation of the unknown (to-be-identified) load vector **f** is shown in Fig 4. For the purpose of identification, it is assumed that the load can occur vertically in 16 points equally spaced along the beam span (vertical axis in Fig. 4). The horizontal axis in Fig. 4 represents the time steps. For clarity of presentation, the first 100 time steps are shown: in such a case, the unknown vector **p** in Eqn (4) has a total of 16 x 100 = 1600 components to be identified.

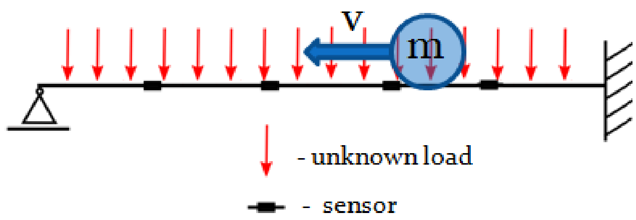


**FIGURE 3.** Scheme of the beam excited by a travelling mass. The load is identified in 16 equally spaced points, and the response is measured by 4 sensors

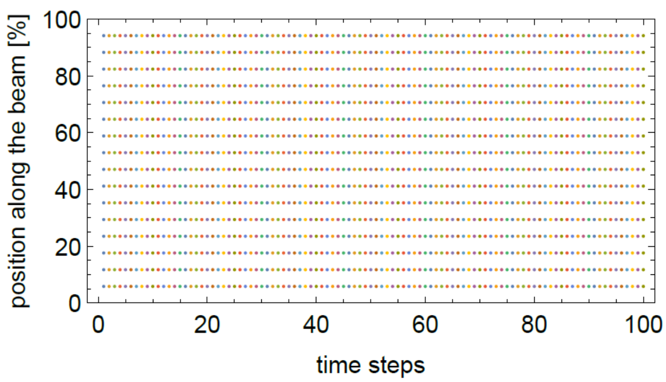


**FIGURE 4.**Graphical representation of the unknown load **f**. The load can occur vertically in 16 points × 100 time steps

Fig.5 presents three exemplary identification results obtained by means of the L1packv2 [11] and Wolfram Mathematica. The provided plots compare the actually simulated and identified trajectories. One and two moving mass loads are simulated. Their actual trajectories are marked by the orange curves, while the identification result is shown in background in the form of the density plots. A good qualitative agreement is evident.

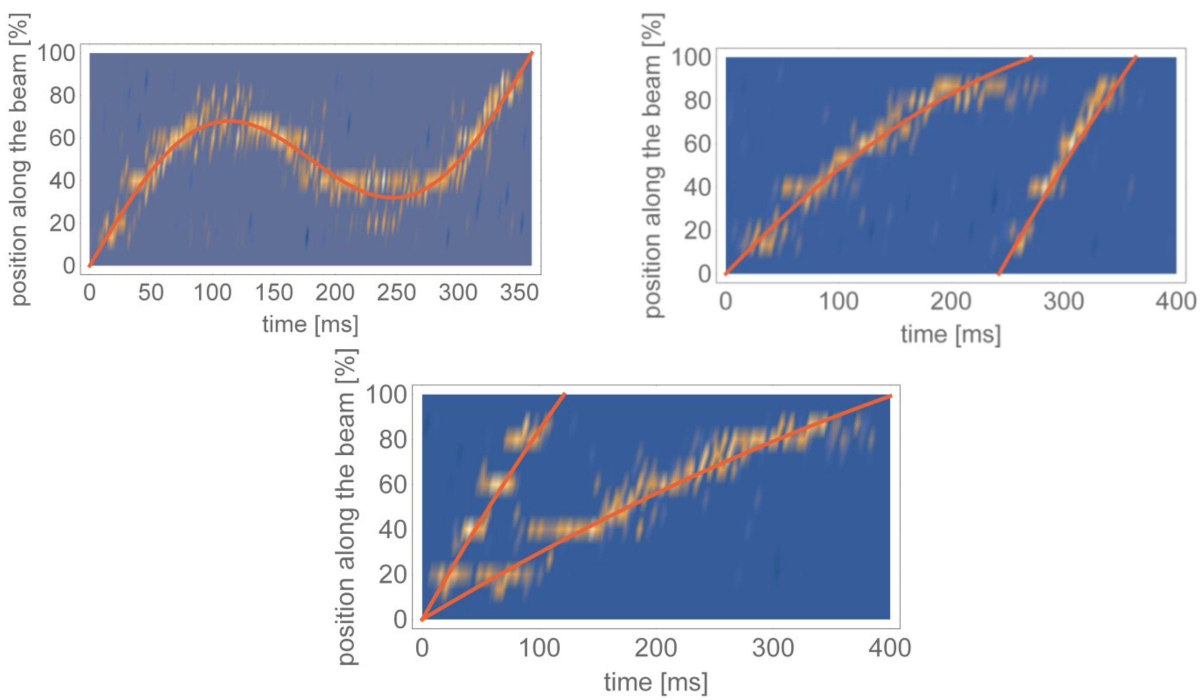


**FIGURE5.** Numerical example: identification of a single moving load and of two moving loads

## EXPERIMENTAL STAND

The experimental stand consists of two parts: a measuring section and a ramp used in order to accelerate the travelling load, see Fig. 6. The measuring section is built to measure strains in selected points of a simply supported beam loaded by a moving mass. The beam has the form of a steel plate (0.55m x 0.03m x .0015m) with a fixed support on the beginning and a rolling support on the end. The beam with supports is installed on thick wall steel profiles, see Fig. 6a. The moving mass is simulated by a steel roller. The roller has a groove on its diameter to provide guidance when travelling along the beam (Fig. 6b). The moving mass is accelerated on the ramp with an adjustable angle, which allows to get various speeds of the moving mass.

The structural response due to the moving mass is measured in nine equally spaced points along the beam by strain gauges, see Fig. 6c. A half-bridge is used and active gauges are installed on the bottom surface of the beam. The compensated strain gauges are installed on the separate steel plate with the same geometry to eliminate the temperature influence. On the beginning and on the end of the measuring section photogates are installed in order to record the start and the end time points of the travelling mass, which is needed to properly determine the part of the measurement from the entire test when the travelling mass actually excited the beam. Additionally, these optical sensors are used to determine the speed of the travelling mass.

The experimental stand allows to record the strain response for singular and multiple masses with different velocities. The strain gauge amplifier contains 8 independent channels. Seven of them are used to measure the strain response in chosen points, while one is used to identify the start and the end moment when the travelling mass enters and leaves the measuring section. The test starts when the travelling mass is located on the ramp and ends when the travelling mass is outside the measuring section. All 8 channels are synchronized and start recording signal in the same time. Strain response could be recorded with the max 2kHz frequency sampling.

Figure 7 shows a comparison between numerical and experimental responses from 4 sensors located at 20%, 40%, 60% and 70% of the beam length. The plots exhibit a satisfying correlation of 93.7% between the results.

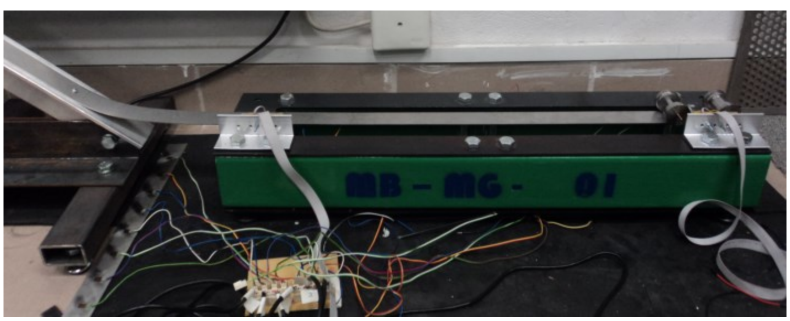


(a)

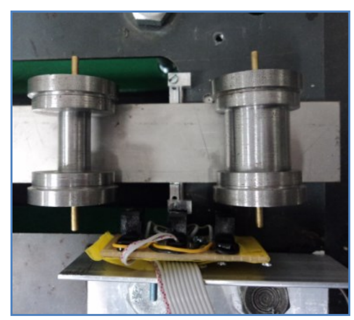

(b)

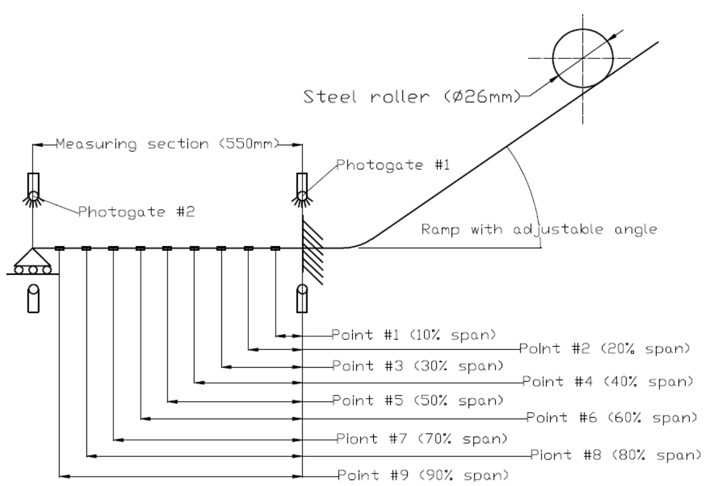


(c)

**FIGURE 6.**The experimental stand: (a) front view, (b) top view with two different mass rollers, (c) schematic draft

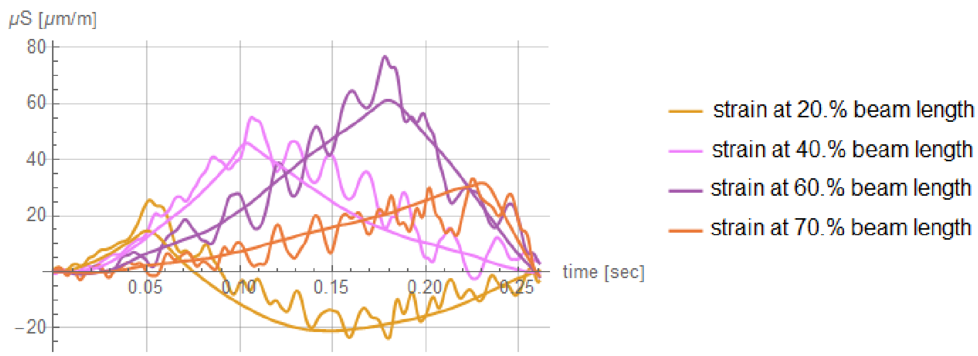


**FIGURE 7.**Comparison of numerical and experimental beam responses in 4 points (20%, 40%, 60% and 70% of the beam length). The smooth lines represent numerical simulations and the oscillatory lines represent the experimental responses. The plot presents only the time section in which the travelling mass is on the measuring section

# EXPERIMENTAL RESULTS

## Single Moving Load

The good qualitative agreement of the numerical results allows us to proceed with experimental verification using the experimental setup described above. The test was carried out with a single mass (156.3g) travelling with two different velocities (1.2m/s and 2.9m/s). Sensors are located at 20%, 40%, 60% and 70% of the beam span. The strain gauge response was recorded with 2kHz sampling frequency. The identification with this sampling frequency is computationally very time consuming. Due to this reason, a downsampling with different ratios was considered. Fig. 8 presents the density plot with the identified trajectory of a single mass with downsampling ratio 10 (200Hz). For the purpose of identification, as in the numerical example described above, the beam FE model is divided into 22 elements and the unknown loads are identified in 16 equally spaced points.

The qualitative agreement between the identified and actual trajectories is noticeably worse than in the case of the purely numerical results. The reason is that the experimental response includes measurement noise, as well as additional errors due to manufacturing tolerances and due to the measurement setup itself. In the numerical identification, only the 10% rms Gaussian noise is taken into account, but there is no variation of the beam geometry and the noise-free signals are assumed to be accurate. A numerically simulated strain gauge provides a pointwise response, while a real gauge averages the strain over its active length (3 mm in our setup). Manual installation of the gauges introduces also position and orientation errors. All these factors contribute to the worsening of the qualitative agreement between the identified and actual trajectories in the case of the lab experiment.

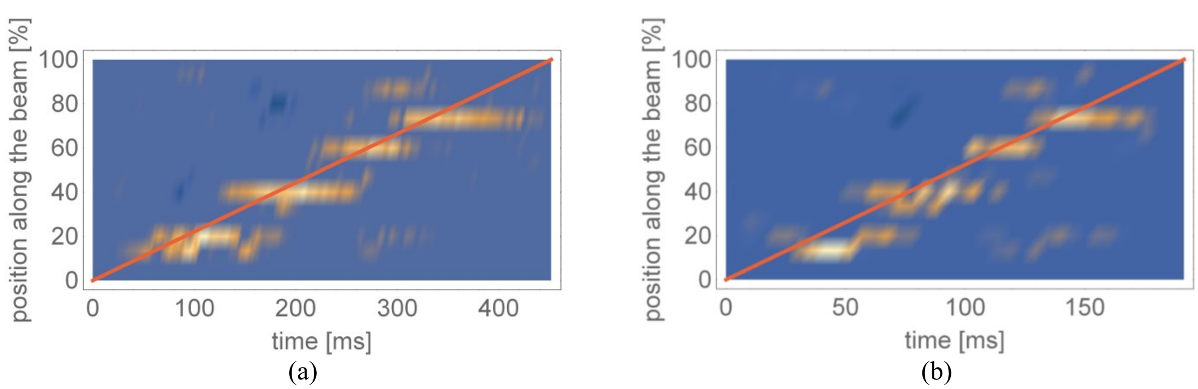


**FIGURE 8**Trajectory identification of a single mass travelling with the average velocity of (a) 1.2m/s and (b) 2.9m/s. The sampling frequency is 200Hz (downsampling ratio 10)

## Sensitivity Study

The experimental setup and the measuring method have a significant impact on the quality of identification results. Modification of the experimental setup is relatively difficult. However, strain gauges are inexpensive and commonly used sensors in structural engineering.

The quality of travelling load identification is also influenced by the software input configuration. The number of the sensors and their placement, the number of load excitation points and the downsampling ratio are assumed a priori. For comparison, Fig.9 shows the identification results with the downsampling ratio 2. In comparison to the results shown in Fig. 8 (downsampling ratio 10), the downsampling ratio has no visible qualitative effect on the identification results but the computational time is significantly increased. Also, increasing the number of the load excitation points from 16 to 40 does not improve the identification quality (see Fig.10). A better result is obtained for additional sensors (see Fig.11). In this configuration, five sensors are installed at 20%, 40%, 60%, 70% and 90% of the beam span. A significant impact of the sensor pattern can be also noticed. Fig 12 shows the identification results obtained with four sensors positioned at 10%, 30%, 70%, and 90% of the beam span. There is a significant decrease in the qualitative agreement in comparison to the original pattern of four sensors shown in Fig. 9.

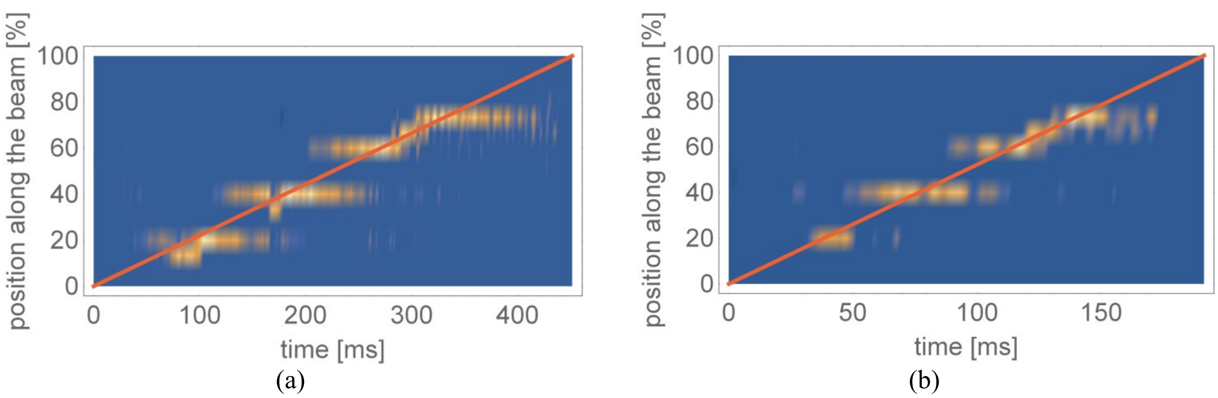


**FIGURE 9.** Trajectory identification of a single moving mass with 1kHz sampling frequency (downsampling ratio 2). Two different velocities considered: (a) 1.2m/s and (b) 2.9m/s

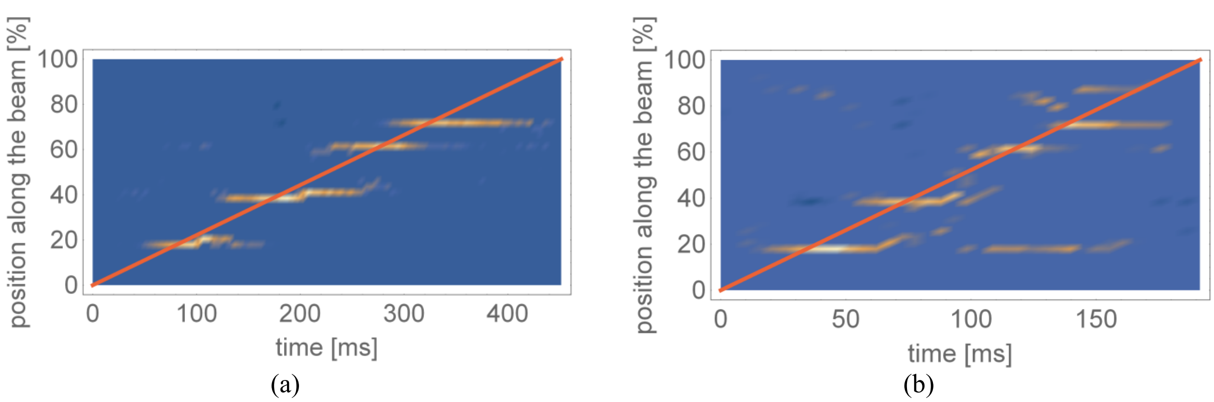


**FIGURE 10.** Trajectory identification of a single moving mass with 40 load excitation points. Two different velocities considered: (a) 1.2m/s and (b) 2.9m/s

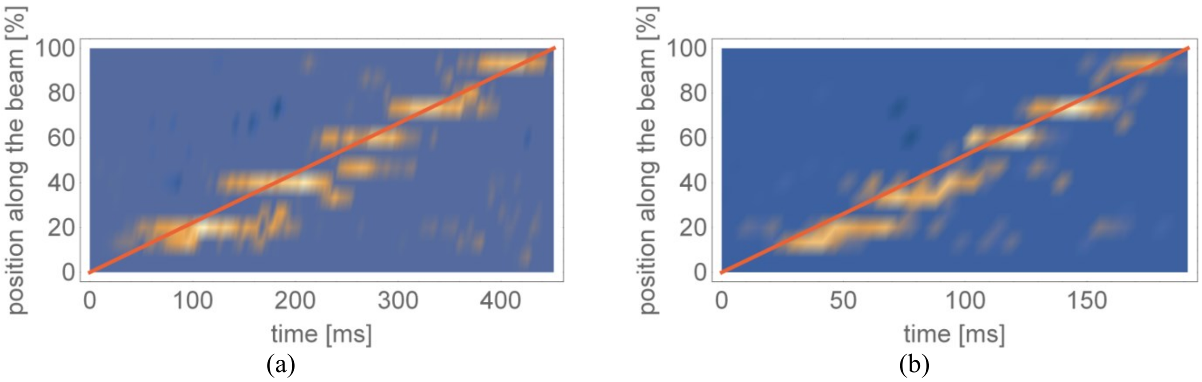


**FIGURE 11.** Trajectory identification of a single moving mass with five sensors installed at 20%, 40%, 60%, 70% and 90% of the beam span. Two different velocities considered: (a) 1.2m/s and (b) 2.9m/s

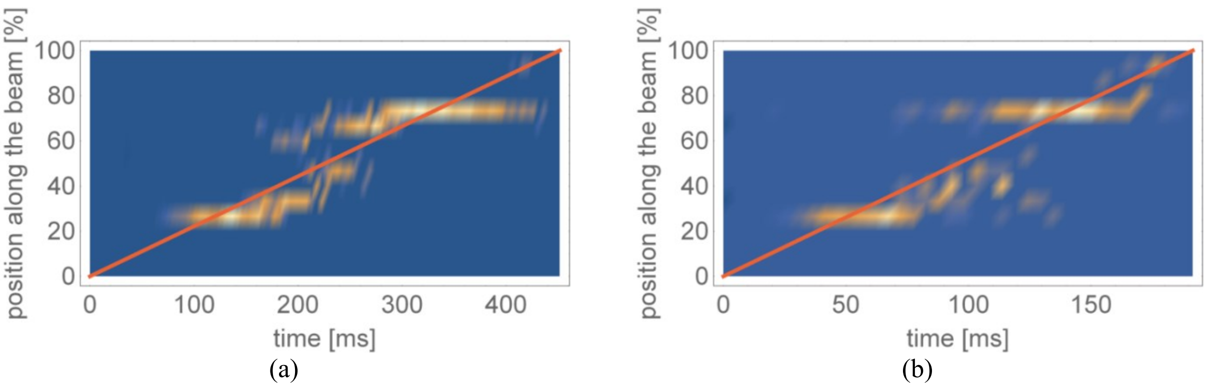


**FIGURE 12.** Trajectory identification of a single moving mass with a different sensor pattern (four sensors placed at 10%, 30%, 70%, and 90% of the beam span). Two different velocities considered: (a) 1.2m/s and (b) 2.9m/s

## CONCLUSIONS

This contribution proposes a method for identification of freely moving loads. The method allows to evaluate underdetermined problems, in which a very large number of DOF scan be excited by the load, but a limited number of sensors are available to measure the response. The approach is based on the assumption of sparsity of the excitation which can be expressed through the $l_1$ norm minimization.

The identified trajectories show a good qualitative agreement with the actual trajectories at 0.31 data redundancy ratio (5 sensors and 16 load points) for experimental results and 0.25 for numerical results (4 sensors and 16 load points). It is confirmed that the sensor placement pattern has a significant impact on the quality of identification. Thus, sensor placement will be optimized in the future to improve the identification results.

The current version of the approach does not consider any additional apriorical knowledge about the load except the sparsity. We plan to determine other specific characteristics of travelling loads in order to exploit them in the process of identification.

## ACKNOWLEDGMENTS

Support of the National Science Centre, Poland, granted through the project Ad-DAMP (DEC-2014/15/B/ST8/04363), is gratefully acknowledged.

## REFERENCES

[1] L. Yu and T. Chan, J. Sound Vib. **305**, 3–21 (2007).
[2] X. Q. Zhu and S. S. Law, J. Civil Struct. Health Monit. **6**, 107–128 (2016).
[3] B.-J. Ryu and Y.-S. Kong, in *Advances on Analysis and Control of Vibrations – Theory and Applications*, edited by M. Zapateiro and F. Pozo (InTech, 2012), pp. 231–250.
[4] X. Q. Zhuand S. S. Law, Adv. Struct. Eng. **18**, 1999–2015 (2015).
[5] Y. Yu, C. S. Caiand L. Deng, Adv. Struct. Eng. **19**, 1514–1530 (2016).
[6] Q. Zhang, Ł. Jankowski, and Z. Duan, Math. Probl. Eng. **2013**, 963424 (2013).
[7] D. Donoho, IEEE T. Inform. Theory **52**, 1289–1302 (2006).
[8] S. Nagarajaiah and Y. Yang, Struct. Control HealthMonit. **24**, e1851 (2017).
[9] B. Qiao, X. Zhang, J. Gao, and X. Chen, J. Sound Vib. **376**, 72–94 (2016).
[10] R. Tibshirani, J. R. Stat. Soc. Ser. B-Stat. Methodol. **73**, 273–282 (2011).
[11] I. Loris, Comput.Phys. Commun. **179**, 895–902 (2008).